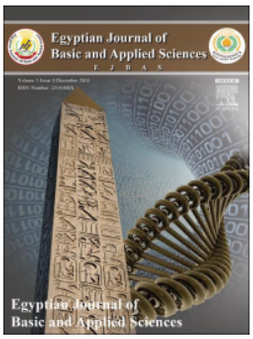

Egyptian Journal of Basic and Applied Sciences

ISSN: 2314-808X (Online) Journal homepage: www.tandfonline.com/journals/teba20

Histological, histochemical, and immunohistochemical changes in mouse pancreas induced by electromagnetic field (EMF) exposure and potential protective effects of crocin

Salma S. Nassar, Marwa S. M. Mahmoud, Somaia A. Negm & Amr M. Abd El-Hady

To cite this article: Salma S. Nassar, Marwa S. M. Mahmoud, Somaia A. Negm & Amr M. Abd El-Hady (2025) Histological, histochemical, and immunohistochemical changes in mouse pancreas induced by electromagnetic field (EMF) exposure and potential protective effects of crocin, Egyptian Journal of Basic and Applied Sciences, 12:1, 638-653, DOI: 10.1080/2314808X.2026.2676359

To link to this article: https://doi.org/10.1080/2314808X.2026.2676359

Published online: 20 May 2026.

EGYPTIAN JOURNAL OF BASIC AND APPLIED SCIENCES
2025, VOL. 12, NO. 1, 638–653
https://doi.org/10.1080/2314808X.2026.2676359

ORIGINAL ARTICLE

OPEN ACCESS Check for updates

Histological, histochemical, and immunohistochemical changes in mouse pancreas induced by electromagnetic field (EMF) exposure and potential protective effects of crocin

Salma S. Nassar[a], Marwa S. M. Mahmoud[b], Somaia A. Negm[c] and Amr M. Abd El-Hady[d]

[a]Zoology Department, Faculty of Science, Zagazig University, Zagazig, Egypt; [b]Department of Zoology, Faculty of Science, Benha University, Benha, Egypt; Coordinator of the Molecular Biology and Biotechnology Program, Obour Campus, Faculty of Science, Benha University, Egypt; [c]Medical Laboratory Technology Department, Faculty of Applied Health Science Technology, Misr University for Science and Technology (MUST), Giza, Egypt; [d]Radiology and Medical Imaging Technology Department, Faculty of Applied Health Science Technology, Misr University for Science and Technology (MUST), Giza, Egypt

ABSTRACT

The widespread use of mobile phones and other devices emitting non-ionizing electromagnetic fields (EMF) has raised concerns about potential biological effects on metabolically active organs such as the pancreas. This study investigated the histological, histochemical, and immunohistochemical effects of EMF exposure and the protective role of crocin in mice. Twenty adult male Swiss albino mice were divided into four groups: control, crocin-treated (20 mg/kg), EMF-exposed (1 h/day for 8 weeks), and crocin-pretreated plus EMF-exposed. Pancreatic tissues were examined using hematoxylin and eosin, Masson's trichrome, and insulin immunohistochemistry, with quantitative image analysis. EMF exposure induced marked pancreatic injury, including acinar cell necrosis, islet degeneration, inflammatory infiltration, hemorrhage, and increased collagen deposition, accompanied by a significant reduction in insulin immunoexpression. In contrast, crocin pretreatment significantly attenuated these histological alterations, reduced collagen accumulation, and improved insulin expression toward near-normal levels. These findings demonstrate that EMF exposure induces structural and functional pancreatic damage, while crocin exerts a protective effect likely related to its antioxidant and cytoprotective properties. However, the lack of biochemical oxidative stress markers limits mechanistic interpretation. Overall, crocin shows potential as a protective agent against EMF-induced pancreatic injury.

ARTICLE HISTORY
Received 24 December 2025
Accepted 14 May 2026

KEYWORDS
Pancreas; mobile phone; histopathology; collagen; insulin; crocin

Introduction

Electromagnetic Radiation (EMR) emitted by various sources, such as mobile phones, has become a significant source of environmental contamination due to the production of non-ionizing radiation (NIR), which may affect different organs and their functions [1]. Especially in developed countries, the use of Wi-Fi and radiation-emitting wireless devices has increased markedly in recent decades [2,3]. Nowadays, the widespread use of modern communication devices, such as mobile phones and Wi-Fi technology, along with a sedentary lifestyle, has raised increasing

CONTACT Amr M. Abd El-Hady amr.elsayed@must.edu.eg Radiology and Medical Imaging Technology Department, Faculty of Applied Health Sciences Technology, Misr University for Science and Technology (MUST), P.O. Box 77, Giza, Egypt

debate about the possible health effects of these devices [4,5].

The rapid proliferation of wireless communication technologies has made human exposure to EMF a continuous and inevitable phenomenon in modern life. Recent experimental findings indicate that chronic EMF exposure can trigger oxidative imbalances, cellular stress responses, and specific structural damage within various tissues, with a pronounced impact on metabolically active organs [6–11], including the pancreas [12–15].

Saffron, the dried stigmas of *Crocus sativus* flowers, is an ancient and highly valued spice that has been used by humans for over 3000 years for flavoring and coloring food and for its unique medicinal properties [16]. Some studies have demonstrated the protective effects of aqueous saffron extract against cyto- and genotoxicity [17]. This raises the question of which specific bioactive constituents of saffron are responsible for these effects. Crocin (CRO), safranal, and picrocrocin are widely recognized as the main bioactive ingredients of saffron [18]. The pancreas is a metabolically active organ with high oxidative susceptibility, making it particularly vulnerable to environmental stressors. To date, numerous studies have been conducted, but the available literature regarding the effects of mobile phone radiation on the pancreas remains limited, and hence the present study. In addition, this work seeks to clarify the potential protective role of crocin against RF-induced pancreatic injury.

The aim of the present study was to investigate the histopathological, histochemical, and immunohistochemical effects of prolonged exposure to mobile phone – derived EMF on the pancreas of mice. However, the present study focuses primarily on histological and immunohistochemical alterations and does not include direct biochemical assessment of oxidative stress markers, which represents an important limitation in mechanistic interpretation.

Materials and methods

Chemicals

Crocin, a water-soluble carotenoid derived from *Crocus sativus* (saffron) and *Gardenia jasminoides*, is the main pigment of saffron and forms red crystalline compounds with the chemical structure shown in (Figure 1) [19].

The crocin used in this study was obtained as a solid powder (molecular weight: 976.96 g/mol; molecular formula: $C_{44}H_{64}O_{24}$). Crocin was obtained from Sigma-Aldrich (St. Louis, MO, USA; Catalog No. C2260, ≥98% purity). It was dissolved in distilled water for oral administration at a dose of 20 mg/kg b.w./day [20].

Animals

Twenty adult male Swiss albino mice, aged 8 weeks and weighing approximately 25–30 g (±10%), were obtained from the Animal Breeding House of the National Research Center, Cairo, Egypt. The animals were maintained under controlled environmental conditions (23–25°C; 12-h light/12-h dark cycle) for one week prior to experimentation for acclimatization. A standard commercial diet and tap water were provided *ad libitum*. All animals were comparable in age, body weight, and general health status at baseline, and random allocation to groups was performed to minimize selection bias.

Although the sample size per group ($n = 5$) may appear limited, it was selected based on prior evidence from comparable experimental histopathological studies evaluating EMF-induced tissue alterations in rodents, where similar group sizes have been widely validated. A priori power estimation based on previously reported effect sizes in similar models indicated that $n = 5$ per group was enough to detect significant differences in histological and immunohistochemical outcomes at $\alpha = 0.05$ with 80% power. This approach ensured adequate statistical sensitivity while maintaining compliance with the ethical principle of reduction (3Rs) in

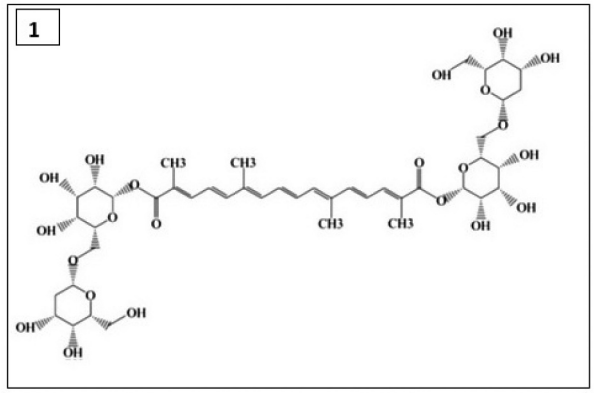

Figure 1. Chemical structure of crocin.

animal experimentation. Furthermore, ethical considerations to minimize animal use were strictly followed in accordance with institutional guidelines. All procedures were approved by the Institutional Animal Care and Use Committee. Ethical approval was obtained from the Experimentation Ethics Committee of Zagazig University prior to the start of the study (Approval number: ZU-IACUC/1/F/451/2023). All procedures involving animals were conducted in strict accordance with institutional ethical guidelines and internationally accepted standards for the care and use of laboratory animals.

Treatment protocol

The mice were randomly divided into four groups ($n = 5$): Group 1 (Control; Sham-exposed) animals were placed in the exposure chamber for 1 hour/day with the EMF-emitting device switched off and received equivalent volumes of distilled water via sham gavage to control for handling and administration-induced stress; Group 2 (Crocin) animals received crocin at a dose of 20 mg/kg b.w. via oral gavage daily for 8 weeks to assess the compound's effects in isolation; Group 3 (EMF-exposed) animals were exposed to EMF radiation within the chamber for 1 hour/day over 8 weeks while receiving daily sham gavages of distilled water to ensure identical handling conditions; and Group 4 (Crocin + EMF - exposed) animals were pretreated with crocin (20 mg/kg b.w.) for one week, followed by daily EMF exposure (1 hour/day) alongside continued crocin administration for 8 weeks to evaluate its protective efficacy.

The dose of crocin (20 mg/kg b.w.) was selected based on established pharmacological data demonstrating its optimal antioxidant efficacy and tissue-protective properties in rodent models without inducing systemic toxicity [21,22]. This specific concentration has been previously shown to effectively neutralize reactive oxygen species and preserve the structural integrity of the pancreas under chemical and environmental stress [22]. The 8-week duration of administration was chosen to parallel the chronic EMF exposure period, ensuring sustained antioxidant bioavailability during the progressive development of potential cellular alterations [23].

EMF exposure protocol

Whole-body EMF exposure was conducted using a standardized mobile phone handset (Nokia 105; SAR = 1.50 W/kg; frequency range 900–1800 MHz). To minimize confounding stress factors, animals were placed in custom-designed, rectangular plexiglass cages (20 × 15 × 15 cm) featuring multiple 0.5 cm

ventilation ports on all sides to allow free airflow and prevent hyperthermia. The EMF source was positioned centrally 2 cm beneath the base of the cage. The device was maintained in a continuous 'active answering mode' for the duration of the 1-hour daily exposure session to ensure a consistent radiation field.

The SAR estimation of 1.50 W/kg represents the peak spatial-average SAR as specified by the manufacturer and is consistent with the experimental configurations validated in previous literature for whole-body exposure in small rodents [24]. The 1-hour exposure duration was chosen to simulate high-intensity, chronic usage patterns, a protocol previously shown to induce detectable histopathological changes in metabolically active tissues [6].

The exposure setup was standardized across all experimental sessions to ensure consistency in positioning, distance, and duration of exposure, and all animals were maintained under identical environmental conditions to minimize variability. However, real-time dosimetric measurements, field strength mapping, and frequency verification were not performed in the current study. Therefore, EMF exposure parameters were based on manufacturer-reported specifications, which may limit precise characterization of the exposure intensity. This represents a methodological limitation that may affect reproducibility and inter-study comparability. Future studies are recommended to incorporate calibrated EMF measurement systems and dosimetric validation techniques to ensure accurate quantification of exposure parameters.

Histological, histochemical, and immunohistochemical studies

For histological, histochemical, and immunohistochemical analyses, all animals were anesthetized with intraperitoneal sodium thiopental (50 mg/kg) [25], then sacrificed at the end of the exposure period. The pancreas was dissected and immediately fixed in 10% neutral buffered formalin for 24 h. Fixed tissues were then processed through graded ethanol dehydration, cleared in xylene, and embedded in paraffin wax. Serial sections (3–4 µm thick) were obtained, deparaffinized, rehydrated, and stained with:

- A. Hematoxylin & eosin according to the method of Bancroft and Gamble [26] for general histological evaluation
- B. Masson's trichrome according to Pearse [27] to assess collagen deposition
- C. Insulin immunostaining using the peroxidase-labeled streptavidin – biotin technique as described by Kiernan [28].

For immunohistochemical analysis, tissue sections were incubated for 1 hour at room temperature with a mouse monoclonal anti-insulin primary antibody (clone 2D11-H5, Cat. No. MA5-12037; Thermo Fisher Scientific, Waltham, MA, USA; formerly Lab Vision Corp.) at a concentration of 0.5–1.0 µg/mL. Microscopic examination and photodocumentation were performed using a digital imaging system (Olympus® SC100 camera) coupled with an Olympus® CX31 light microscope (Japan). All experimental procedures were conducted at the Faculty of Science, Zagazig University, Egypt. To minimize observer bias, all sections were evaluated in a blinded manner by an experienced pathologist who was unaware of the group allocation.

Morphometric assessment

ImageJ software (version 1.47, USA) was used to measure the optical density of insulin-secreting β-cells. Ten non-overlapping fields were randomly selected from five representative images (×200) per experimental group. All images were acquired under identical microscope settings (illumination, contrast, and magnification) to ensure standardization. Image calibration was performed using a stage micrometer prior to

analysis to ensure measurement accuracy. Image selection and quantitative analysis were performed independently by two observers who were blinded to the experimental groups to minimize observer bias. Re-analysis of a subset of samples was performed to assess reproducibility, showing minimal variability. Inter-observer variability was evaluated and demonstrated a high level of agreement (intraclass correlation coefficient, ICC > 0.85). Mean optical density (MOD) values were calculated for each group and used for statistical analysis.

Statistical analysis

Statistical analysis was performed using the Statistical Package for the Social Sciences (SPSS), version 20 for Windows (SPSS/PC). Data were expressed as mean ± standard deviation (SD) for each experimental group ($n = 5$). Differences among groups were evaluated using one-way analysis of variance (ANOVA), followed by Tukey's post-hoc multiple comparison test. Pairwise comparisons were conducted between all groups, including direct comparison between the EMF-exposed group and the EMF + Crocin group to specifically assess the protective effect of crocin. A p-value ≤ 0.05 was considered statistically significant, while $p \leq 0.01$ was regarded as highly significant. Significant differences compared to the control (sham-exposed) group were indicated by an asterisk (*).

Prior to parametric analysis, data distribution was assessed using the Shapiro – Wilk test to verify normality, while homogeneity of variances was evaluated using Levene's test to ensure validity of ANOVA assumptions. To strengthen statistical rigor and transparency, effect sizes (eta-squared, η^2) were calculated for all comparisons to quantify the magnitude of observed differences beyond p-values alone. Given the relatively small sample size ($n = 5$ per group), statistical interpretation was performed cautiously, and results were supported by both p-values and effect size estimates to reduce the risk of Type I and Type II errors.

Results

Histopathological observations

Light microscopic examination of pancreatic sections from the Control (Sham-exposed) group demonstrated a typical histological architecture. The pancreatic lobules were clearly defined, consisting of densely packed exocrine acini with pyramidal cells exhibiting basal basophilic nuclei and apical acidophilic cytoplasm. Interspersed within the acinar tissue were well-organized, pale-staining islets of Langerhans with distinct cellular boundaries (Figure 2 / 2, 3). Similarly, the Group 2 (Crocin) animals showed no histological abnormalities; the pancreatic parenchyma in this group was histologically indistinguishable from the Control (Sham-exposed) group, preserving the integrity of both the exocrine and endocrine components without evidence of inflammatory infiltration or necrosis (Figure 2/4).

However, the pancreas of the EMF-exposed mice (1 h of exposure per day for 8 weeks) showed several histopathological alterations in both the exocrine and endocrine components. The exocrine acinar cells appeared necrotic and degenerative, while the islet cells appeared shrunken and damaged, with no clear demarcation between the exocrine and endocrine portions. Marked lymphocytic infiltration in both compartments was observed, suggesting a form of pancreatitis, accompanied by hemorrhage, congested blood vessels, and cytoplasmic vacuolization. The interlobular septa exhibited dilated and congested blood vessels and a pancreatic duct lined with destructed epithelial cells (Figure 3/5, 6).

Examination of other pancreatic sections from the EMF-exposed group showed a more advanced stage of atrophy of the necrotic pancreatic acini, which appeared severely degenerated, with associated hemorrhage. The islets of Langerhans appeared poorly defined, with extensively destructed cells or almost completely lost, leaving large vacuoles and an irregular boundary. The border between the exocrine and endocrine portions became highly indistinct and irregular (Figure 4/7, 8).

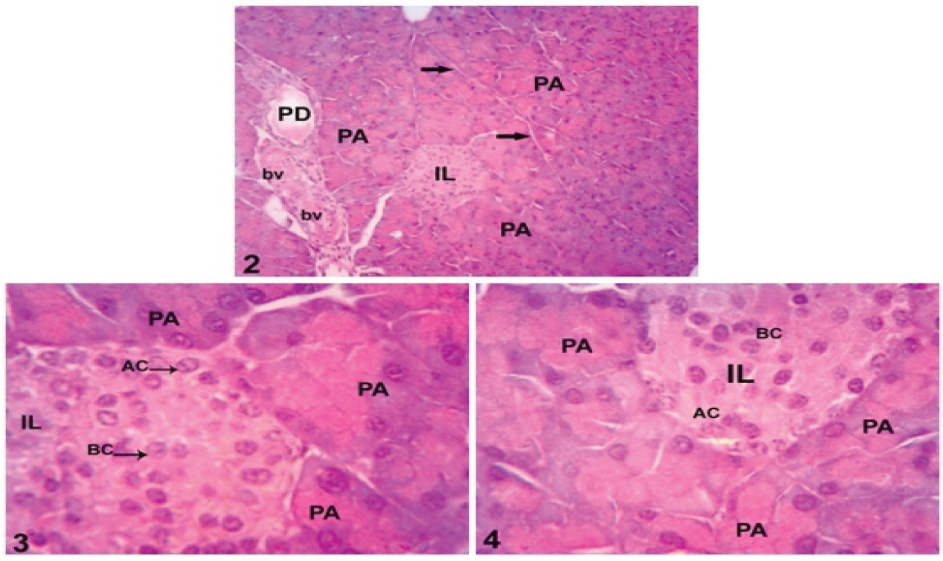

Figure 2. Histopathological features of control and crocin-treated pancreas (H&E). (2) a pancreatic section from the control (sham-exposed) group (H&E, magnification × 400) demonstrates a typical histological layout, with pancreatic acini (PA) organized into lobules separated by interlobular septa (arrows) and exhibiting normally pale-staining islets of Langerhans (il), along with visible interlobular pancreatic ducts (pd) and blood vessels (bv). (3) higher magnification of the same tissue (magnification × 1000) reveals more intensely stained PA composed of pyramidal cells with basophilic nuclei and apically acidophilic cytoplasm, in addition to clearly showing the cellular elements of the islets of Langerhans, including alpha-cells (ac) and beta-cells (BC). (4) a pancreatic section from the G2 (Cro-administered) group (H&E, magnification × 1000) shows a normal histological pattern closely comparable to the control, preserving the normal architecture of the PA and il, with identifiable ac and BC.

On the other hand, animals in the Cro + EMF group exhibited clear signs of partial cellular regeneration in the pancreatic parenchyma, including both the pancreatic acini (PA) and the islets of Langerhans (IL), indicating notable histological improvement following crocin supplementation. Most acinar cells showed intact basophilic nuclei and apical acidophilic cytoplasm, although some vacuolization persisted. The islets of Langerhans also demonstrated partial restoration, containing recognizable alpha and beta cells, while focal necrotic areas and vacuolization remained detectable. The residual atrophic changes in both acinar and islet cells were less pronounced, and the border separating the exocrine and endocrine portions appeared more distinct and regular along most of its course (Figure 5/9, 10).

Histochemical observations

Collagen

Assessment of collagen distribution in the pancreatic tissue of the control (sham-exposed) and crocin-treated groups showed a weak (+) reaction, evidenced by light green staining with Masson's trichrome. Collagen fibers were mainly observed within the connective tissue septa separating the pancreatic lobules, outlining the islets of Langerhans, and within the interstitial tissue (Figure 6/11, 12). In contrast, EMF-exposed mice exhibited a marked increase in collagen fiber deposition in the same regions (Figure 7/13, 14). Notably, mice pretreated with crocin prior to irradiation demonstrated a substantial reduction in collagen accumulation, approaching the near-normal pattern observed in the control group (Figure 7/15).

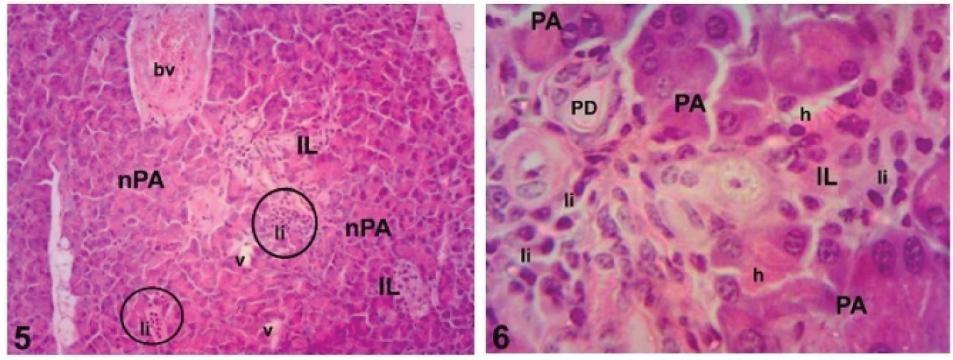

Figure 3. Histopathological alterations in the EMF-exposed group (H&E). (5) Section of the pancreas from G3 (RF-irradiated group) (1 h/day for 8 weeks) (H&E, magnification × 400) showing degenerated and necrotic pancreatic acini (nPA), shrunken islet of Langerhans (il). Notice the lymphocytic infiltration (li) involving both the exocrine and endocrine portions. The interlobular septa show a congested blood vessel (bv) and cytoplasmic vacuolization (v). No clear demarcation is observed between the exocrine and endocrine regions. (6) enlarged portion of the previous pancreatic section from the irradiated group (H&E, magnification × 1000) showing damaged pancreatic acini (PA), hemorrhage (h), and an islet of Langerhans (il) with degenerated cells surrounded by lymphocytic infiltration (li). A pancreatic duct (pd) with destructed epithelial cells is also observed.

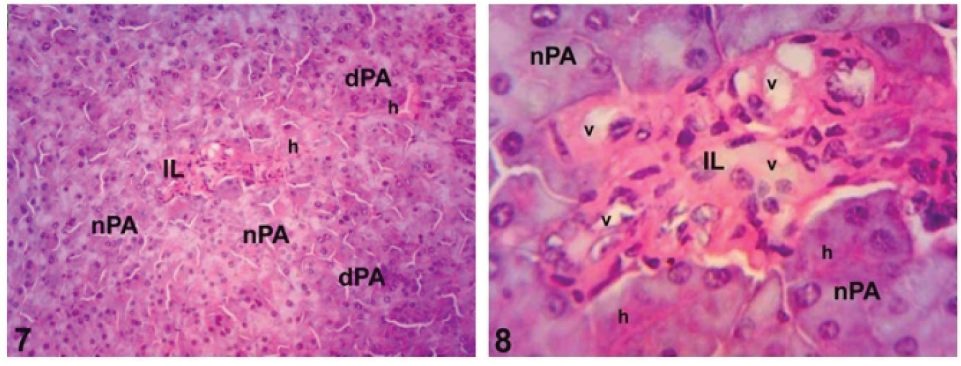

Figure 4. Advanced atrophic changes in the EMF-exposed group (H&E). (7) Section of pancreas from another animal in G3 (RF-irradiated group) (1 h/day for 8 weeks) (H&E, magnification × 400) showing marked atrophic changes in the pancreatic acini, which appear severely degenerated and necrotic (dPA, nPA), with associated hemorrhage (h). The islet of Langerhans (il) appears ill-defined, with destructed cells and an irregular outline. (8) magnified portion of the previous section from the irradiated group (magnification × 1000) showing a marked atrophic stage of the necrotic pancreatic acini (nPA) with associated hemorrhage (h). The islet of Langerhans (il) shows severely destructed cells or is almost completely lost, leaving large vacuoles (v). The border between the exocrine and endocrine portions has become indistinct and irregular.

Immunohistochemical observations

Insulin immunoexpression

Concerning the immunohistochemical distribution of insulin-secreting β-cells, the islets of Langerhans in both the control (sham-exposed) group and crocin-treated groups demonstrated strong, intense brown cytoplasmic immunoreactivity (Figure 8/ 16, 17). Quantitative analysis of the images showed mean optical density (MOD) values of 0.70 ±

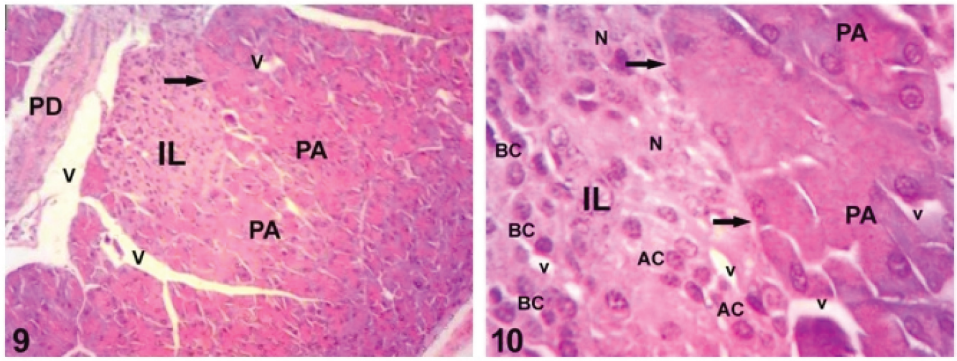

Figure 5. Effects of crocin on EMF-induced injury (H&E). (9) Section of pancreas from G4 (Cro + RF-irradiated) (1 h/day for 60 days) (H&E, magnification x400) showing mild regeneration in both the exocrine and endocrine portions, except for the presence of vacuoles (v). The border between the exocrine and endocrine regions became more distinct and regular along part of its course (arrow). PA: pancreatic acini, il: islets of Langerhans, pd: pancreatic duct, v: vacuoles. (10) magnified portion of the previous section (magnification × 1000) showing a clear regenerative phase attributed to crocin supplementation. Most pancreatic acini (PA) display intact basophilic nuclei and apical acidophilic cytoplasm, except for areas of vacuolization (v). The islets of Langerhans (il) show partial regeneration, with some intact alpha cells (ac) and beta cells (BC), while necrotic areas (N) and vacuolization (v) are still evident.

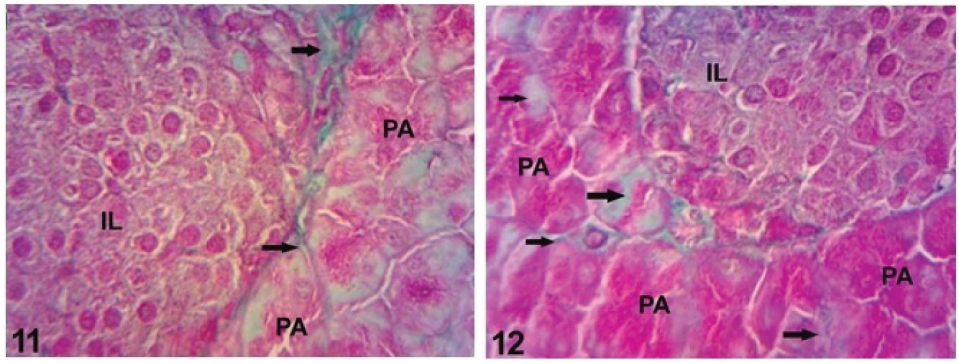

Figure 6. Collagen distribution in control and crocin groups (Masson's trichrome). (11) Section of pancreas from the control (sham-exposed) group (Masson's trichrome stain, magnification × 1000) showing a weak (+) deposition of collagen fibers in the extracellular spaces, particularly within the connective tissue between the pancreatic acini (PA) and the islets of Langerhans (il). (12) Section of pancreas from the crocin-administered group (Masson's trichrome stain, magnification × 1000) showing a weak (+) collagen fiber deposition in the pancreatic parenchyma, closely resembling the control (sham-exposed) group. Pancreatic acini (PA) and islets of Langerhans (il) appear normal. Arrows indicate the connective tissue septa between pancreatic lobules.

0.08 for the control (sham-exposed) group and 0.71 ± 0.04 for the crocin-treated group (Table 1, Figure 10). By contrast, the EMF-exposed group exhibited shrunken islets with markedly reduced insulin immunoexpression, with only a few β-cells showing weak positivity (Figure 9 / 18), which corresponded to a significant decrease in MOD (0.55 ± 0.03;

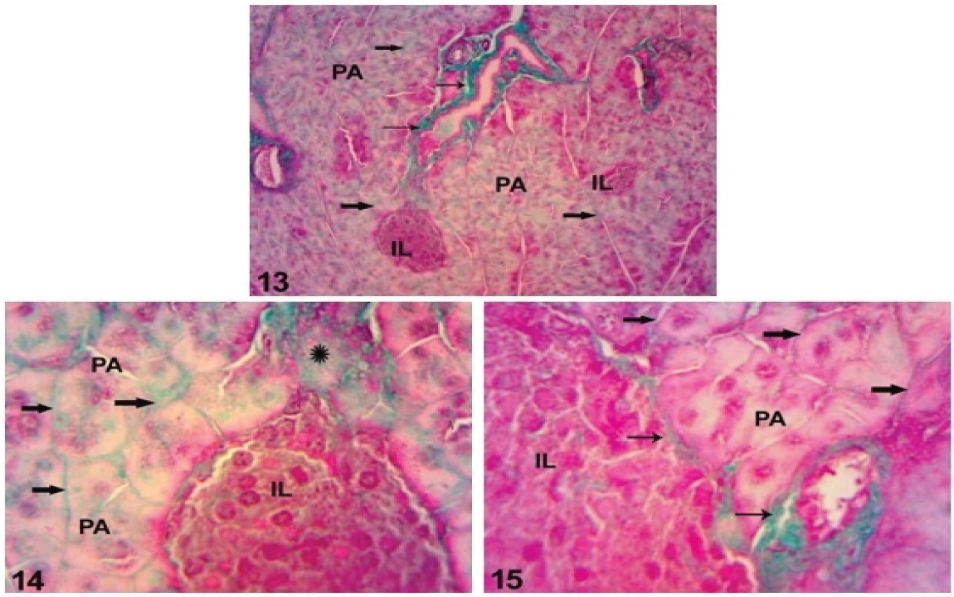

Figure 7. Impact of EMF and crocin on collagen deposition (Masson's trichrome). (13) Section of pancreas from the RF-irradiated group (Masson's trichrome stain, magnification × 400) showing a moderate (++) increase in collagen deposition within the pancreatic acini (PA) and islet cells (il) (thick arrows), along with a strong (+++) reaction in the connective tissue surrounding the intercalated and intralobular ducts (thin arrows). (14) Section of pancreas from the RF-irradiated group (Masson's trichrome stain, magnification × 1000) showing a moderate (++) increase in collagen deposition within the pancreatic acini (PA) and islet cells (il) (thick arrows), along with a strong (+++) reaction in the connective tissue surrounding the intercalated ducts (*). (15) Section of pancreas from the Cro + RF-irradiated group (Masson's trichrome stain, magnification × 1000) showing a weak (+) reaction in the pancreatic acini (PA) and islet cells (il) (thick arrows) and a moderate (++) reaction in the connective tissue of intercalated ducts and the connective tissue between islet cells and the exocrine portion (thin arrows).

$p \leq 0.05$) compared to controls (Table 1, Figure 10). Moreover, the remaining islets in EMF-exposed mice displayed irregular architecture compared to the normal structure observed in unexposed controls (Figure 8 / 16).

Importantly, the crocin-pretreated EMF-exposed group showed substantial preservation of insulin immunoreactivity, demonstrated by the increased number of positively stained β-cells (Figure 9 / 19). This protective effect was supported by a significant increase in MOD (0.63 ± 0.04; $p \leq 0.05$) relative to the EMF-exposed group, approaching the control values (Table 1, Figure 10). Additionally, the number of insulin-positive β-cells was noticeably greater in crocin-pretreated irradiated mice than in those exposed to irradiation without crocin pretreatment.

Discussion

Mobile phone – related non-ionizing EMF fields have been widely investigated for their potential biological effects beyond thermal mechanisms. Preclinical evidence indicates that chronic or repeated EMF exposure can disrupt pancreatic structure and function through oxidative stress, inflammation, and early fibrotic changes [29,30]. Experimental studies in rodents and isolated islets have further shown that EMF exposure impairs insulin secretion [31],

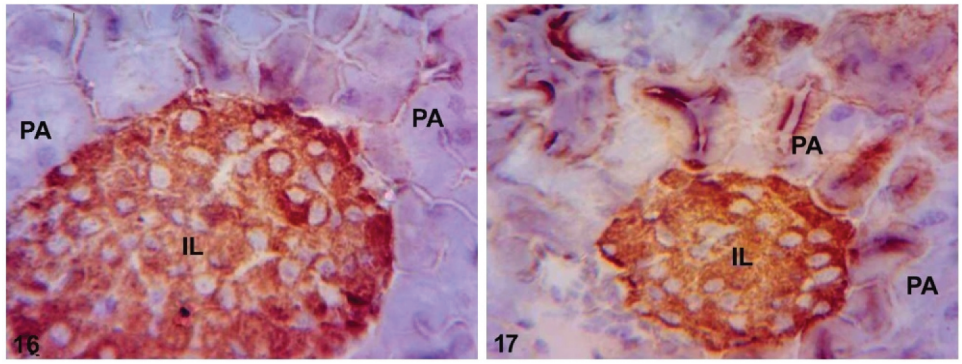

Figure 8. Insulin expression in control and crocin groups (IHC). (16) insulin-immunostained section of the pancreas from the control (sham-exposed) group (magnification × 1000) showing strong brown cytoplasmic immunopositive reaction in the β-cells of the islets of Langerhans (il), surrounded by normal pancreatic acini (PA). (17) Section of the pancreas from group 2 (crocin-administered) mice (insulin immunostaining, magnification × 1000) showing insulin immunoexpression comparable to the control (sham-exposed) group, with strong cytoplasmic positivity in β-cells of the islets of Langerhans (il).

Table 1. Mean optical density (MOD) of insulin immunohistochemical expression in the pancreas.

Groups	Mean Optical Density of (MOD)	Significance vs Control	Significance vs EMF
Control	0.70 ± 0.08	–	–
Crocin	0.71 ± 0.04	NS	–
EMF-exposed	0.55 ± 0.03	*$p \leq 0.05$	–
Crocin + EMF-exposed	0.63 ± 0.04	*$p \leq 0.05$	#$p \leq 0.05$

Data are expressed as mean ± standard deviation (SD) ($n = 5$ per group). Statistical analysis was performed using SPSS (version 20, IBM, USA). Intergroup differences were analyzed using one-way ANOVA followed by Tukey's post-hoc test after verification of normality and homogeneity of variance. A p-value ≤ 0.05 was considered statistically significant. Effect sizes were estimated to assess the magnitude of differences between groups. The symbol (*) indicates a significant difference compared with the control group, while (#) indicates a significant difference compared with the EMF-exposed group. NS = not significant.

elevates oxidative stress biomarkers [32], and promotes inflammatory cell infiltration with extracellular matrix collagen deposition in pancreatic tissue [33].

It is important to note that oxidative stress biomarkers (such as malondialdehyde (MDA), superoxide dismutase (SOD), catalase (CAT), and reduced glutathione (GSH)) were not assessed in the present study. Accordingly, any interpretation related to oxidative stress should be considered indirect and based on morphological and immunohistochemical correlates rather than direct biochemical evidence. Therefore, the suggested antioxidant mechanism of crocin is based on previously published experimental evidence rather than direct biochemical measurements in this work. Future studies incorporating oxidative stress assays are recommended to confirm this proposed mechanism. In the present study, chronic EMF exposure resulted in significant histopathological, histochemical, and immunohistochemical alterations in the pancreas, affecting both exocrine and endocrine components. Previous studies have suggested that elevated oxidative stress and associated disruptions of cell membranes are major contributors to EMF-induced cellular damage [34]. Furthermore, microwaves emitted from mobile phones can increase free radical formation, enhance lipid peroxidation, and alter antioxidant defenses, ultimately leading to oxidative injury [35]. In addition, long-term mobile phone use has been reported to

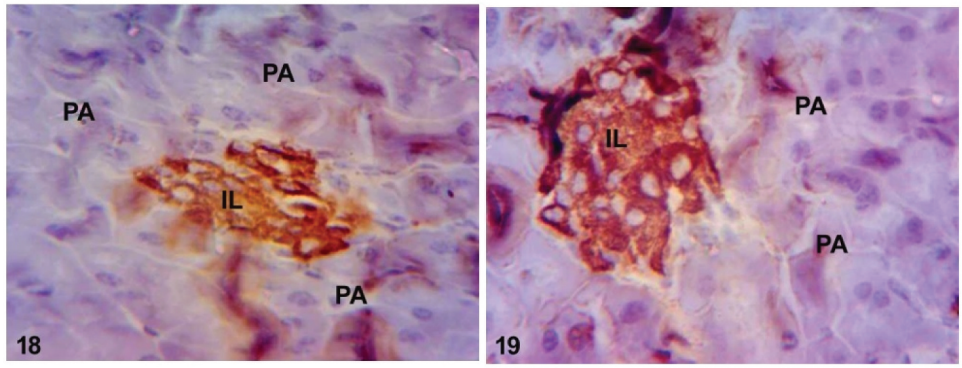

Figure 9. Impact of EMF and crocin on insulin immunoexpression (IHC). (18) Section of the pancreas from G3 (RF-irradiated group) (insulin immunostaining, magnification × 1000) showing markedly decreased insulin immunoreactivity in a shrunken and damaged islet of Langerhans (il). Note the irregular morphology of the residual islet cells. Surrounding pancreatic acini (PA) are also observed. (19) Section of the pancreas from G4 (crocin + RF-irradiated group) (insulin immunostaining, magnification × 1000) showing partial regeneration in the previously damaged islet of Langerhans (il) and surrounding pancreatic acini (PA), with an increase in insulin immunoreactivity compared to the irradiated group alone. PA: pancreatic acini.

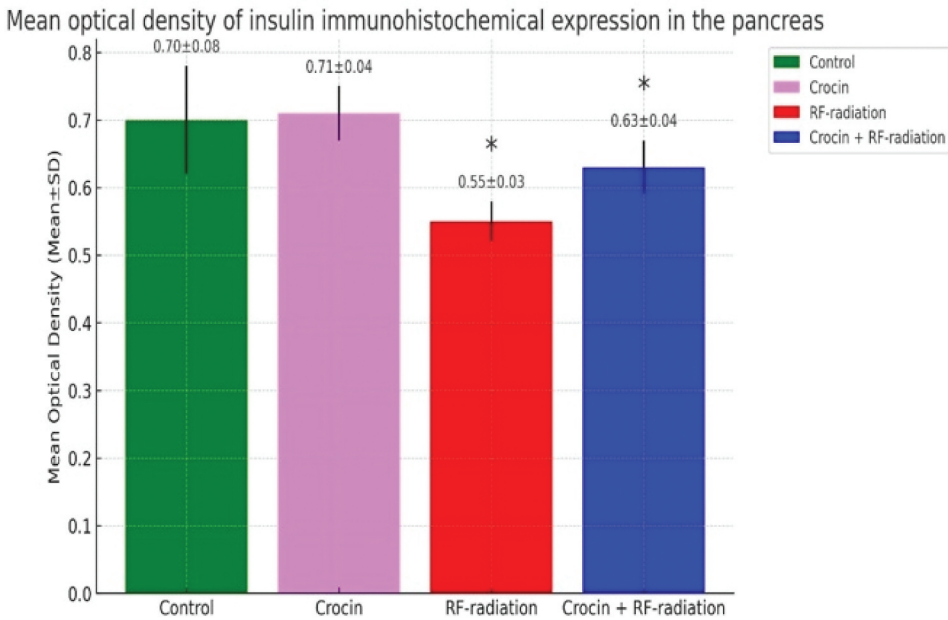

Figure 10. Showing the mean optical density of insulin immunohistochemical expression in different experimental groups.

induce inflammation in the liver and pancreatic cells of albino rats compared to matched controls [36]. Similarly, prolonged exposure of rats to EMF (50 Hz, 24 h/day) for 135 days was shown to impair insulin secretion by altering the structure of the endocrine pancreas [37]. These findings are consistent with previous reports indicating that EMF-induced oxidative stress contributes to cellular injury, inflammation, fibrosis, and β-cell dysfunction [38,39].

In the current work, normal pancreatic architecture was preserved in the control (sham-exposed) group and crocin-treated groups, with intact acinar structures and well-organized islets of Langerhans showing strong insulin immunoexpression. In contrast, EMF-exposed mice exhibited marked degeneration of acinar cells, necrosis, cytoplasmic vacuolation, and intense inflammatory infiltration. Severe distortion of islet architecture, loss of β-cell mass, and poor exocrine – endocrine demarcation was also evident. Similar morphological disturbances following EMF exposure have been reported [40]. These findings collectively support the sensitivity of pancreatic tissue, particularly β-cells, to EMF-induced structural injury. Importantly, this study provides the first integrated histological, histochemical, and immunohistochemical evaluation of EMF-induced pancreatic injury alongside crocin-mediated recovery within a single experimental model, offering a comprehensive structural – functional correlation and establishing baseline data for future mechanistic studies.

The increased collagen deposition observed in the EMF group confirms chronic inflammation – associated fibrotic responses. Notably, crocin pretreatment markedly reduced collagen accumulation, supporting its antifibrotic and anti-inflammatory properties [41]. Similar observations were reported in rat thyroid tissue, where collagen deposition was attributed to a direct response of the thyroid gland to EMF [42]. This aligns with findings observing collagen deposition following 8 weeks of exposure to EMF radiation in Masson's trichrome-stained thyroid sections, particularly within septa between thyroid lobules and follicles, following 8 weeks of exposure to EMF, as observed under light and electron microscopy [43]. Fibrotic remodeling has been attributed in previous studies to oxidative stress – mediated activation of transforming growth factor beta (TGF-β), a key regulator of extracellular matrix deposition [44,45]. Although TGF-β signaling was not directly assessed in the current study, the observed increase in collagen deposition is consistent with activation of profibrotic pathways reported in previous literature.

Insulin immunohistochemistry revealed a significant reduction in β-cell insulin expression in EMF-exposed mice, indicating impaired β-cell viability and function. The decrease in MOD values reflects reduced insulin synthesis, which may predispose to glucose intolerance or diabetes-like changes. Similar EMF-induced β-cell dysfunction has been previously reported and linked to oxidative stress – mediated impairment of pancreatic endocrine signaling [46,47]. In the present work, crocin supplementation improved β-cell preservation and partially restored insulin immunoreactivity. These findings are in line with crocin's antioxidant, cytoprotective, and antidiabetic effects, attributed to ROS scavenging, mitochondrial protection, and anti-apoptotic modulation [48–50]. Importantly, the partial restoration of insulin immunoreactivity suggests functional recovery of β-cells rather than purely structural preservation.

Crocin's protective role against pancreatic tissue injury is further supported by studies showing that it mitigates oxidative damage, downregulates pro-inflammatory cytokines, and enhances pancreatic tissue regeneration [51,52]. The partial restoration of islet architecture improved acinar cell integrity, reduced collagen content, and enhanced insulin expression in the Cro + EMF group indicate that crocin can counteract EMF-induced pancreatic injury and promote tissue recovery. Pancreatic β-cells are highly susceptible to oxidative stress due to their limited antioxidant defense systems despite producing high levels of reactive oxygen species (ROS) [53]. Persistent ROS exposure suppresses insulin gene expression and reduces insulin release [54]. This creates a vicious cycle whereby oxidative stress diminishes insulin synthesis, and the resulting insulin deficiency further

increases ROS generation, worsening β-cell damage [55].

A major limitation of the present study is the absence of direct measurement of oxidative stress biomarkers such as MDA, SOD, CAT, and GSH. Therefore, the proposed antioxidant mechanism of crocin remains speculative and is inferred from previously published studies rather than experimentally confirmed in the current model. This limitation restricts definitive mechanistic conclusions and highlights the need for integrated biochemical validation in future studies.

The present work is primarily descriptive, focusing on histological, histochemical, and immunohistochemical alterations. The absence of molecular and biochemical markers, such as inflammatory cytokines (e.g. TNF-α, IL-6) and apoptosis-related proteins (e.g. caspase-3, Bcl-2), limits mechanistic depth and reduces the ability to fully elucidate the underlying pathways. Future studies integrating biochemical and molecular analyses are warranted to strengthen causal interpretation.

Additionally, the EMF exposure conditions were not validated using real-time dosimetry or frequency measurements, which may affect reproducibility and precise characterization of exposure intensity. Although standardized manufacturer specifications were followed, the absence of independent dosimetric verification represents a methodological limitation.

The mechanistic interpretations presented in this study are based on previously published evidence and should be considered inferential rather than definitive, as the current experimental design does not directly investigate molecular pathways. Despite these limitations, the study provides consistent morphological and immunohistochemical evidence supporting a protective role of crocin against EMF-induced pancreatic injury.

Conclusion

Crocin confers significant protection against EMF-induced pancreatic injury in mice, as demonstrated by integrated histopathological, histochemical, and immunohistochemical evidence, including preservation of tissue architecture and partial restoration of insulin immunoexpression.

While these findings are consistent with the established antioxidant and cytoprotective properties of crocin, the absence of direct biochemical and molecular measurements (e.g. oxidative stress markers, inflammatory cytokines, and apoptosis-related pathways) limits definitive mechanistic interpretation.

Nevertheless, this study provides novel multi-level morphological evidence of pancreatic injury and recovery under EMF exposure, establishing a robust experimental baseline for future investigations. Further studies incorporating validated dosimetry, quantitative molecular analyses, and long-term safety evaluation are required to clarify mechanisms and support translational relevance in humans.

Disclosure statement

No potential conflict of interest was reported by the author(s).

Availability of data and materials

The data can be made available from the corresponding author on reasonable request.

Consent to publish

All authors have read the submitted manuscript and consent to its publication.

References

[1] Boris Đ, Dušan S, Dejan K, et al. Biochemical and histopathological effects of mobile phone exposure on rat hepatocytes and brain. Acta Med Medianae. 2010;49:37–42.

[2] Kumar SBJ, Sisodia R. Influence of electromagnetic fields on reproductive system of male

rats. Int J Radiat Biol. 2013;89(3):147–154. doi: 10.3109/09553002.2013.741282

[3] Naziroglu M, Yuksel M, Ozkaya MO, et al. Wi-Fi and mobile phone radiation–induced oxidative stress and reproductive signaling alterations. J Membr Biol. 2013;246(12):869–875. doi: 10.1007/s00232-013-9597-9

[4] Swerdlow AJ, Feychting M, Green AC, et al. Mobile phones, brain tumors, and the Interphone study. Environ Health Perspect. 2011;119(11):1534–1538. doi: 10.1289/ehp.1103693

[5] Kismali G, Ozgur E, Guler G, et al. Effects of 1800 MHz GSM signals on blood chemistry and oxidative stress in rabbits. Int J Radiat Biol. 2012;88(5):414–419. doi: 10.3109/09553002.2012.661517

[6] Nassar SA, Emam NM, Eid FA, et al. Non-ionizing radiation–induced ultrastructural retinal changes. J Am Sci. 2011;7(12):1196–1208.

[7] Nassar SA, Algazeery A, Sayed Ahmed GA, et al. Chronic mobile phone RF radiation induces testicular alterations in immature mice. Egypt J Hosp Med. 2020;78(1):128–135. doi: 10.21608/ejhm.2020.68482

[8] Gurhan H, Bajtoš M, Barnes F. Weak radiofrequency field effects on chemical parameters that characterize oxidative stress in human fibrosarcoma and fibroblast cells. Biomolecules. 2023;13(7):1112. doi: 10.3390/biom13071112

[9] Lai H, Levitt BB. Cellular and molecular effects of non-ionizing electromagnetic fields. Rev Environ Health. 2023;39(3):519–529. doi: 10.1515/reveh-2023-0023

[10] Meyer F, Bitsch A, Forman HJ, et al. The effects of radiofrequency electromagnetic field exposure on biomarkers of oxidative stress in vivo and in vitro: a systematic review of experimental studies. Environ Int. 2024;194:108940. doi: 10.1016/j.envint.2024.108940

[11] Wang S, Yang J, Zhen C, et al. Electromagnetic fields regulate iron metabolism: from mechanisms to applications. J Adv Res. 2026;80:1155–1177. doi: 10.1016/j.jare.2025.04.044

[12] Sakurai T, Yoshimoto M, Koyama S, et al. Elf magnetic fields affect insulin-secreting cells. Bioelectromagnetics. 2008;29(2):118–124. doi: 10.1002/bem.20370

[13] Sakurai T, Terashima S, Miyakoshi J. Mri static magnetic fields affect insulin-secreting cells. Bioelectromagnetics. 2009;30(1):1–8. doi: 10.1002/bem.20433

[14] Gholampour F, Javadifar TS, Owji SM, et al. Prolonged exposure to extremely low frequency electromagnetic field affects endocrine secretion and structure of pancreas in rats. Int J Zool Res. 2011;7(4):338–344. doi: 10.3923/ijzr.2011.338.344

[15] Paraš SD, Gajanin RB, Manojlović ML, et al. Impact of high-frequency electromagnetic fields on secretion and structure of pancreas in rats. In: Eskola, H., Väisänen, O., Viik, J., Hyttinen, J. (eds) European Medical and Biological Engineering Conference. Springer Singapore; 2017. p. 711–714. doi: 10.1007/978-981-10-5122-7_178

[16] Melnyk JP, Wang S, Marcone M. Chemical and biological properties of saffron. Food Res Int. 2010;43(8):1981–1989. doi: 10.1016/j.foodres.2010.07.033

[17] Premkumar K, Abraham SK, Santhiya ST, et al. Saffron extract inhibits chemical genotoxicity in mice. Asia Pac J Clin Nutr. 2003;12:474–476.

[18] Rahaiee S, Moini S, Hashemi M, et al. Antioxidant activities of saffron extracts. J Food Sci Technol. 2015;52(4):1881–1888. doi: 10.1007/s13197-013-1238-x

[19] Ali A, Yu L, Kousar S, et al. Crocin: functional characteristics, extraction, food applications and efficacy against brain related disorders. Front Nutr. 2022;9:1009807. doi: 10.3389/fnut.2022.1009807

[20] Zheng YQ, Liu JX, Wang JN, et al. Crocin protects cerebral microvessels after ischemia. Brain Res. 2007;1138:86–94. doi: 10.1016/j.brainres.2006.12.064

[21] Hosseini A, Razavi BM, Hosseinzadeh H. Pharmacokinetic properties of saffron and its active components. Eur J Drug Metab Pharmacokinet. 2018;43(4):383–390. doi: 10.1007/s13318-017-0449-3

[22] Altinoz E, Turkoz Y, Ekici K, et al. The protective effect of crocin on cisplatin-induced toxicity in rat pancreas. Arh Hig Rada Toksikol. 2015;66(1):37–42. doi: 10.1515/aiht-2015-66-2538

[23] Abdel-Daim MM, Abushouk AI, Ghazy EW, et al. Synergistic protective effects of ceftriaxone and crocin against cisplatin-induced nephrotoxicity in rats. Sci Rep. 2019;9(1):14720. doi: 10.1038/s41598-019-51315-y

[24] Yilmaz H, Tümkaya L, Mercantepe T, et al. Effects of 5G mobile phone network electromagnetic field exposure on testicular endoplasmic reticulum stress and the protective role of coenzyme Q10. Arch Med Res. 2025;56(4):103157. doi: 10.1016/j.arcmed.2024.103157

[25] Bedir Z, Erdem KTO, Can A, et al. Thiamine pyrophosphate protects against metamizole liver injury. Int J Pharmacol. 2023;19 (1):139–146. doi: 10.3923/ijp.2023.139.146
[26] Bancroft J, Gamble M. Theory and practice of histological techniques. 7th ed. London: Churchill Livingstone; 2008.
[27] Pearse A. Histochemistry: theoretical and applied. 3rd ed. London: Churchill Livingstone; 1977.
[28] Kiernan J. Immunohistochemistry. In: Bancroft JD, Gamble M (eds) Histological and histochemical methods. 4th ed. Banbury: Scion Publishing; 2015. p. 454–490.
[29] Leung PS, Chan YC. Oxidative stress in pancreatic inflammation. Antioxid Redox Signal. 2009;11(1):135–165. doi: 10.1089/ars.2008.2109
[30] Kilic A, Ustunova S, Bulut H, et al. Prenatal and postnatal 900 MHz EMF exposure induces inflammation and oxidative stress in offspring. Life Sci. 2023;321:121627. doi: 10.1016/j.lfs.2023.121627
[31] Dehaghi BF, Shekarloo MV, Golbaghi A, et al. Electromagnetic field exposure and diabetes: a narrative review. J Environ Health Sust Dev. 2024; 9(4):2390–2404.
[32] Salameh M, Zeitoun-Ghandour S, Sabra L, et al. GSM-EMW exposure alters oxidative stress markers in fetal rat liver. Sci Rep. 2023;13(1):17806. doi: 10.1038/s41598-023-44814-z
[33] Masoumi A, Karbalaei N, Mortazavi SMJ, et al. Wi-Fi radiation impairs insulin secretion in rat pancreatic islets. Int J Radiat Biol. 2018;94 (9):850–857. doi: 10.1080/09553002.2018.1490039
[34] Lahijani MS, Tehrani DM, Sabouri E. Electromagnetic field effects on liver of chicken embryo. Electromagn Biol Med. 2009;28(4):391–413. doi: 10.3109/15368370903287689
[35] Kesari KK, Behari J. Whole-body 900-MHz radiation exposure effects on enzyme activities in male wistar rats. Electromagn Biol Med. 2010;29(1–2):1–10. doi: 10.3109/15368371003683834
[36] Meo SA, Arif M, Rashied S, et al. Mobile phone radiation induces liver and pancreas changes. Eur J Anat. 2010;14(3):105–109.
[37] Gholampour F, Javadifar T, Owji S, et al. ELF-EMF exposure alters pancreatic endocrine function. Int J Zool Res. 2011;7(4):338–400. doi: 10.3923/ijzr.2011.393.400
[38] Newsholme P, Keane KN, Carlessi R, et al. Oxidative stress pathways in pancreatic β-cells. Am J Physiol Cell Physiol. 2019;317(3): C420–C433. doi: 10.1152/ajpcell.00141.2019
[39] Coman LI, Balaban DV, Dumbravă BF, et al. Antioxidant strategies in acute pancreatitis. Nutrients. 2025;17(15):2390. doi: 10.3390/nu17152390
[40] Topsakal S, Ozmen O, Cicek E, et al. Gallic acid ameliorates Wi-Fi–induced pancreatic lesions. J Radiat Res Appl Sci. 2017;10(3):233–240. doi: 10.1016/j.jrras.2017.04.009
[41] Naimi H, Khazaei M, Sharifnia F, et al. Anti-inflammatory and fibrinolytic effects of crocin after tendon injury. J Tradit Complement Med. 2024;14(6):687–696. doi: 10.1016/j.jtcme.2024.06.001
[42] Mohamed DA, Elnegris HM. EMF exposure alters thyroid histology: protective role of vitamin E. J Cytol Histol. 2015;6:374. doi: 10.4172/2157-7099.1000374
[43] Mohamed M, Saleh S, Asaad Amin M, et al. 4G mobile phone radiation affects thyroid histology. Egypt J Histol. 2023;46 (3):1108–1119. doi: 10.21608/ejh.2022.126546.1656
[44] Liu RM, Pravia K. Oxidative stress and glutathione in TGF-β fibrogenesis. Free Radic Biol Med. 2010;48(1):1–15. doi: 10.1016/j.freeradbiomed.2009.09.026
[45] Xavier S, Piek E, Fujii M, et al. Inhibition of TGF-β signaling reduces radiation fibrosis. J Biol Chem. 2004;279(15):15167–15176. doi: 10.1074/jbc.M309798200
[46] Kajimoto Y, Kaneto H. Oxidative stress in pancreatic beta-cell dysfunction. Ann N Y Acad Sci. 2004;1011(1):168–176. doi: 10.1196/annals.1293.017
[47] Khaki AA, Alihemmati A, Nobahari R. Electromagnetic field effects on pancreatic islets and insulin release. 2015. Available from: https://dspace.tbzmed.ac.ir/handle/123456789/48360
[48] Behrouz V, Dastkhosh A, Hedayati M, et al. Crocin improves glycemic control in type 2 diabetes. Diabetol Metab Syndr. 2020;12 (1):59. doi: 10.1186/s13098-020-00568-6
[49] Bastani S, Vahedian V, Rashidi M, et al. Antioxidant and anti-inflammatory effects of crocin. Biomed Pharmacother. 2022;153:113297.
[50] Sánchez-Fernández C, Del Olmo-Aguado S, Artime E, et al. Crocin protects trigeminal neurons from oxidative stress. Molecules. 2024;29 (2):456. doi: 10.3390/molecules29020456

[51] Yaribeygi H, Noroozadeh A, Mohammadi MT, et al. Crocin enhances antioxidant defenses in pancreatic cells. J Pharmacopunct. 2019;22 (2):83–89. doi: 10.3831/KPI.2019.22.010
[52] Zhang L, Jing M, Liu Q. Crocin attenuates inflammation and oxidative stress in diabetic nephropathy. Life Sci. 2021;278:119542.
[53] Wang J, Wang H. Oxidative stress in pancreatic beta-cell regeneration. Oxid Med Cell Longev. 2017;2017(1):1930261. doi: 10.1155/2017/1930261
[54] Kaneto H, Matsuoka T. Oxidative stress suppresses insulin biosynthesis in diabetes. Int J Mol Sci. 2012;13(10):13680–13690. doi: 10.3390/ijms131013680
[55] Chen X, Xie N, Feng L, et al. Oxidative stress in diabetes and its complications. Chin Med J. 2025;138(1):15–27.